# Polysome distribution of phospholipid hydroperoxide glutathione peroxidase mRNA: evidence for a block in elongation at the UGA/selenocysteine codon

J. E. Fletcher, P. R. Copeland and D. M. Driscoll

*RNA* 2000 6: 1573-1584

*RNA* (2000), *6*:1573–1584. Cambridge University Press. Printed in the USA.


# Polysome distribution of phospholipid hydroperoxide glutathione peroxidase mRNA: Evidence for a block in elongation at the UGA/selenocysteine codon

**JULIA E. FLETCHER, PAUL R. COPELAND, and DONNA M. DRISCOLL**
Department of Cell Biology, Lerner Research Institute, Cleveland Clinic Foundation, Cleveland, Ohio 44195, USA

## ABSTRACT

**The translation of mammalian selenoprotein mRNAs requires the 3′ untranslated region that contains a selenocysteine insertion sequence (SECIS) element necessary for decoding an in-frame UGA codon as selenocysteine (Sec). Selenoprotein biosynthesis is inefficient, which may be due to competition between Sec insertion and termination at the UGA/Sec codon. We analyzed the polysome distribution of phospholipid hydroperoxide glutathione peroxidase (PHGPx) mRNA, a member of the glutathione peroxidase family of selenoproteins, in rat hepatoma cell and mouse liver extracts. In linear sucrose gradients, the sedimentation velocity of PHGPx mRNA was impeded compared to CuZn superoxide dismutase (SOD) mRNA, which has a coding region of similar size. Selenium supplementation increased the loading of ribosomes onto PHGPx mRNA, but not CuZn SOD mRNA. To determine whether the slow sedimentation velocity of PHGPx mRNA is due to a block in elongation, we analyzed the polysome distribution of wild-type and mutant mRNAs translated in vitro. Mutation of the UGA/Sec codon to UGU/cysteine increased ribosome loading and protein synthesis. When UGA/Sec was replaced with UAA or when the SECIS element core was deleted, the distribution of the mutant mRNAs was similar to the wild-type mRNA. Addition of SECIS-binding protein SBP2, which is essential for Sec insertion, increased ribosome loading and translation of wild-type PHGPx mRNA, but had no effect on the mutant mRNAs. These results suggest that elongation is impeded at UGA/Sec, and that selenium and SBP2 alleviate this block by promoting Sec incorporation instead of termination.**

**Keywords: mammalian SECIS element; polysome analysis; SECIS binding protein 2 (SBP2); selenocysteine insertion**

## INTRODUCTION

Selenocysteine (Sec) is a unique amino acid important in conferring increased enzymatic activity on a small yet essential family of both prokaryotic and eukaryotic proteins. The Sec residue in most selenoproteins is a pivotal component in catalyzing redox reactions (Low & Berry, 1996; Stadtman, 1996; Gladyshev & Hatfield, 1999). The selenoenzymes that use Sec for its redox potential include the bacterial formate dehydrogenases and the mammalian deiodinases, thioredoxin reductases, and glutathione peroxidases (GPx). One of the glutathione peroxidases, phospholipid hydroperoxide glutathione peroxidase (PHGPx), has multiple functions. One role for PHGPx may be in the enzymatic protection against the formation of atherosclerotic lesions by the removal of pathogenic lipids (Thomas et al., 1990). In addition to a peroxidative role in spermatids (Roveri et al., 1992, 1994), PHGPx can act as a structural protein in the midpiece of the mature spermatozoa by aggregating through di-selenide crosslinks (Ursini et al., 1999). The major emphasis of our studies is to elucidate the mechanism of Sec insertion using PHGPx as a model.

The incorporation of Sec into selenoproteins involves the recoding of a UGA codon that is normally a translational stop codon. The decoding of UGA as Sec requires a distinct and specific RNA structure, but several differences exist between prokaryotes and eukaryotes in the process of this decoding mechanism. The bacterial Sec insertion sequence (b-SECIS) is a stable stem-loop structure found in the coding region of the mRNA immediately 3′ of the UGA/Sec codon (Huttenhofer et al., 1996). Three gene products (*sel*A, *sel*C,

Reprint requests to: Donna M. Driscoll, Department of Cell Biology, Lerner Research Institute, Cleveland Clinic Foundation, 9500 Euclid Ave. #NC-10, Cleveland, Ohio 44195, USA; e-mail: driscod@ccf.org.

and *sel*D) are necessary for synthesizing the Sec-tRNA$^{Sec}$ (Leinfelder et al., 1988; Forchhammer & Bock, 1991; Ehrenreich et al., 1992). The fourth component required for Sec insertion in bacteria is a novel elongation factor (SELB) that forms a complex with the SECIS element and the selenocysteyl-tRNA$^{Sec}$ (Sec-tRNA$^{Sec}$) through specific interactions (Zinoni et al., 1990; Heider et al., 1992; Baron et al., 1993; Chen et al., 1993a). This ternary complex is thought to promote Sec incorporation into the nascent protein by mediating an interaction between the Sec-tRNA$^{Sec}$ and the A site of the ribosome (Heider et al., 1992; Baron et al., 1993).

Unlike the prokaryotic pathway, the mechanism of Sec insertion into eukaryotic selenoproteins is less well defined. Mammalian selenoproteins cannot be expressed in bacteria (Rocher et al., 1991) even though eukaryotic homologs of the tRNA$^{Sec}$ and selenophosphate synthetase that correspond to bacterial *sel*C and *sel*D, respectively, have been isolated (Lee et al., 1989; Kim & Stadtman, 1995; Low et al., 1995). One major difference is the position of the SECIS element, which in mammalian selenoprotein mRNAs is located in the 3′ untranslated region (3′ UTR) far downstream of the UGA/Sec codon (Berry et al., 1991). In mammalian selenoprotein mRNAs, the SECIS element consists of three highly conserved sequences predicted to form a stable stem-loop structure. These sequences include three consecutive, unpaired A residues in the terminal loop, an AUGA in the stem 8–10 nt 5′ of the terminal loop, and a GA in the 3′ region of the stem-loop across from the AUGA element (Berry et al., 1991; Shen et al., 1993). Reported to form non-Watson–Crick base pairs (Walczak et al., 1996, 1998), the AUGA and GA elements create a region termed the SECIS core (Martin et al., 1998). An important component that binds specifically to the SECIS core was recently isolated and characterized by our lab. This SECIS-binding protein, termed SBP2, is required for Sec insertion and increases the efficiency of mammalian selenoprotein translation in vitro (Copeland & Driscoll, 1999; Copeland et al., 2000). SBP2 does not have elongation factor homology, and we have hypothesized that SBP2 may be involved in preventing termination at the UGA/Sec codon. However, the function of SBP2 in Sec incorporation remains to be elucidated.

The efficiency of Sec incorporation is reported to be low in mammalian cells. In transient transfection experiments using type I iodothyronine deiodinase (D1), the level of readthrough at the UGA codon was only ~2% the level of readthrough of a UGU/Cys codon in the same position (Berry et al., 1992). The production of full-length D1 was further reduced by transfecting excess selenoprotein DNA into cells or by growing cells under conditions of limited selenium (Berry et al., 1994). Cotransfection of the Sec-tRNA$^{Sec}$ did increase D1 activity but less than twofold (Berry et al., 1994). These results suggest that certain components in the selenoprotein biosynthetic pathway are limiting in transfected cells. In addition, the availability of selenium in vivo affects PHGPx synthesis at a posttranscriptional level, because depletion of selenium decreased PHGPx protein levels yet had little effect on PHGPx mRNA levels (Lei et al., 1995; Bermano et al., 1996). Recently, we found that SBP2 is limiting for the translation of PHGPx mRNA in vitro in reticulocyte lysates (Copeland et al., 2000). We would like to determine what contributes to the inefficiency of Sec insertion compared to that of the more standard amino acids. Our current model suggests that Sec incorporation entails the modification of translating ribosomes through a signal conferred by a complex of the SECIS element bound to SBP2. This complex, and possibly other *trans*-acting factors, may block termination at the UGA/Sec codon and promote Sec incorporation instead. The inefficient production of selenoproteins may result from a combination of the limited availability of required factors in the complex, coupled with slow rate of insertion when all the components are available.

One way to clarify what is occurring during the synthesis of selenoproteins is to analyze the polysomes that translate their mRNAs. In this study, we analyzed the polysome profile of PHGPx mRNAs in cell extracts, in mouse liver, and in an in vitro translation system. We found that PHGPx mRNA exhibits a slow sedimentation velocity compared to other actively translated mRNAs. The levels of ribosome loading on PHGPx mRNA were increased by selenium supplementation of cells, by mutating the UGA/Sec codon in PHGPx mRNA to UGU/Cys, or by adding SBP2 to the in vitro translation reaction. Our results suggest that there is a defect in elongation at the UGA/Sec codon, either due to the ribosome pausing or termination, and that selenium and SBP2 alleviate this defect by promoting Sec incorporation. These results also provide the first direct evidence that SBP2 increases ribosomal loading on a selenoprotein mRNA.

## RESULTS

### PHGPx mRNA in rat hepatoma cell extracts sediments more slowly than actively translated mRNAs

The sedimentation velocity of cytoplasmic extracts on sucrose gradients has been used to analyze the association of mRNAs and ribosomes (Chen et al., 1993b; Kleene, 1993). The loading of ribosomes onto a specific mRNA depends on the coding region length, as well as the rates of initiation, elongation, and termination. To characterize the polysomes that translate endogenous PHGPx mRNA, cytoplasmic extracts were made from McArdle 7777 cells, a rat hepatoma cell line, which were grown in media containing 5 ng/mL

sodium selenite. The extracts were fractionated on linear sucrose gradients. The absorbance of the gradient was recorded at 254 nm, and total RNAs were isolated from each fraction. The RNAs were analyzed by gel electrophoresis for the 18S and 28S ribosomal RNAs, and by Northern blotting for specific mRNAs. In a typical absorbance profile from McArdle cell extracts, the peaks for the 40S and 60S ribosomal subunits, the 80S monosomes, and polysomes with increasing numbers of ribosomes bound to RNA can be resolved (Fig. 1A).

The Northern blots in Figure 1B show the distribution of the mRNAs that encode PHGPx, glutathione peroxidase (GPx), CuZn superoxide dismutase (SOD), and glyceraldehyde-3-phosphate-dehydrogenase (GAPDH). Both the CuZn SOD and GAPDH mRNAs sedimented in the polysome-rich region of the gradient, which is consistent with these mRNAs being translationally active. Having a coding region of 1 kb, GAPDH mRNA sediments with heavier polysomes in the last fractions of the gradient (Fig. 1B, fractions 15 and 16). CuZn SOD mRNA, which has a 460-nt coding region, peaks in fractions 11–13. Interestingly, even though PHGPx mRNA and CuZn SOD have coding regions of similar size (510 and 460 nt, respectively), the two mRNAs do not cosediment in the gradient. Instead, PHGPx mRNA sediments with a broad distribution in the lighter portion of the gradient, peaking in fractions 9 and 10 in the region where monosomes and disomes sediment (Fig. 1B). When the blot in Figure 1B was stripped and reprobed for another selenoprotein mRNA, GPx, a distribution similar to the PHGPx mRNA was observed even though the GPx coding region is longer (603 nt).

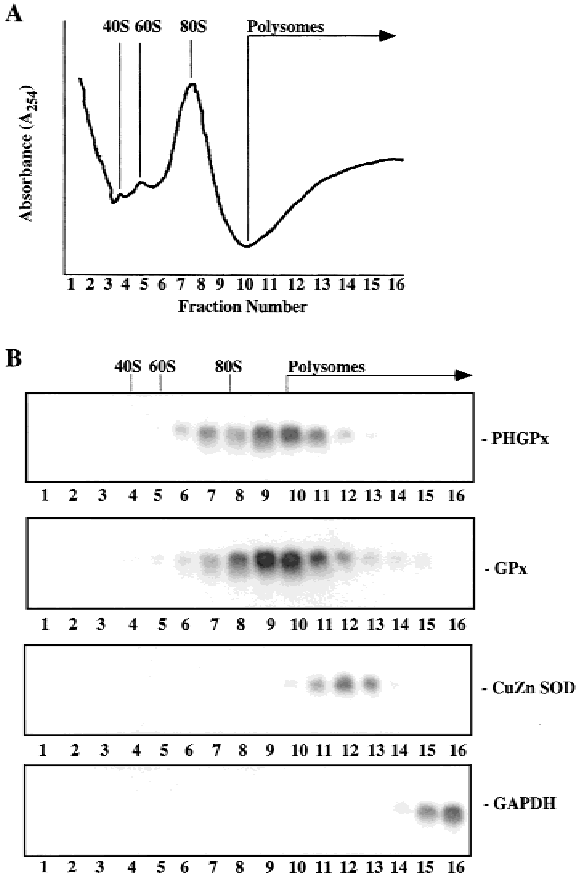


**FIGURE 1.** Polysome distribution of PHGPx mRNA in rat hepatoma cell extracts. **A**: Cytoplasmic extracts from selenium-supplemented McArdle 7777 cells were fractionated in 15–50% (w/v) linear sucrose gradients and collected in 16 fractions. A typical absorbance is shown and the peaks for the positions of the 40S (fractions 3–4) and 60S (fractions 5–6) ribosomal subunits, monosomes (fractions 7–9), and polysomes (fractions 10–16) are indicated. **B**: RNAs extracted from each fraction were analyzed by Northern blotting using probes for PHGPx, GPx, CuZn SOD, and GAPDH mRNAs as indicated. The positions of the ribosomal subunits, monosomes, and polysomes are indicated.

The spacing of ribosomes on the coding region of an actively translated mRNA is approximately every 80–100 bases (Lodish & Jacobson, 1972; Palmiter, 1972; Lodish & Porter, 1980; Meyuhas et al., 1987). The distribution of PHGPx mRNA to the lighter portion of the gradient does not correlate with the loading of 5 to 6.5 ribosomes, which would be predicted for its 510 nt coding region if the mRNA was fully loaded. More consistent with our sedimentation results is the association of PHGPx mRNA with a smaller complex of 1–2 ribosomes. This number of ribosomes could be accommodated on 135 nt, which is the distance between the initiator AUG and the UGA/Sec codon in PHGPx mRNA. The GPx mRNA also has 135 nt between the translation start site and the UGA/Sec codon. These results suggests that elongation may be impeded at the UGA/Sec codon in selenoprotein mRNAs.

### Selenium supplementation increases loading of the ribosomes on PHGPx mRNA

To determine if selenium supplementation increases the loading of ribosomes onto PHGPx mRNA, McArdle 7777 cells were grown in media containing 5 ng/mL sodium selenite (Se+) or without supplementation (Se−). We found that selenium supplementation substantially increased PHGPx protein levels based on western blot analysis, but had no effect on PHGPx mRNA levels (data not shown). The polysomes from the (Se−) and (Se+) cells were analyzed in two separate gradients, which were fractionated in parallel, and the gradient fractions were analyzed by Northern blotting for PHGPx and CuZnSOD mRNAs (Fig. 2A). The results were quantified by PhosphorImager analysis, and the percent distribution of each mRNA was plotted. This experiment was repeated twice with similar results. Compared to (Se+) cells where PHGPx mRNA peaks in fraction 10, PHGPx mRNA in (Se−) cells sediments in the lighter region of the gradient, peaking in fraction 8. The shift of PHGPx mRNA to the heavier portion of the gradient is a specific effect, as selenium supplementation did not significantly affect the distribution of CuZn SOD mRNA (Fig. 2B).

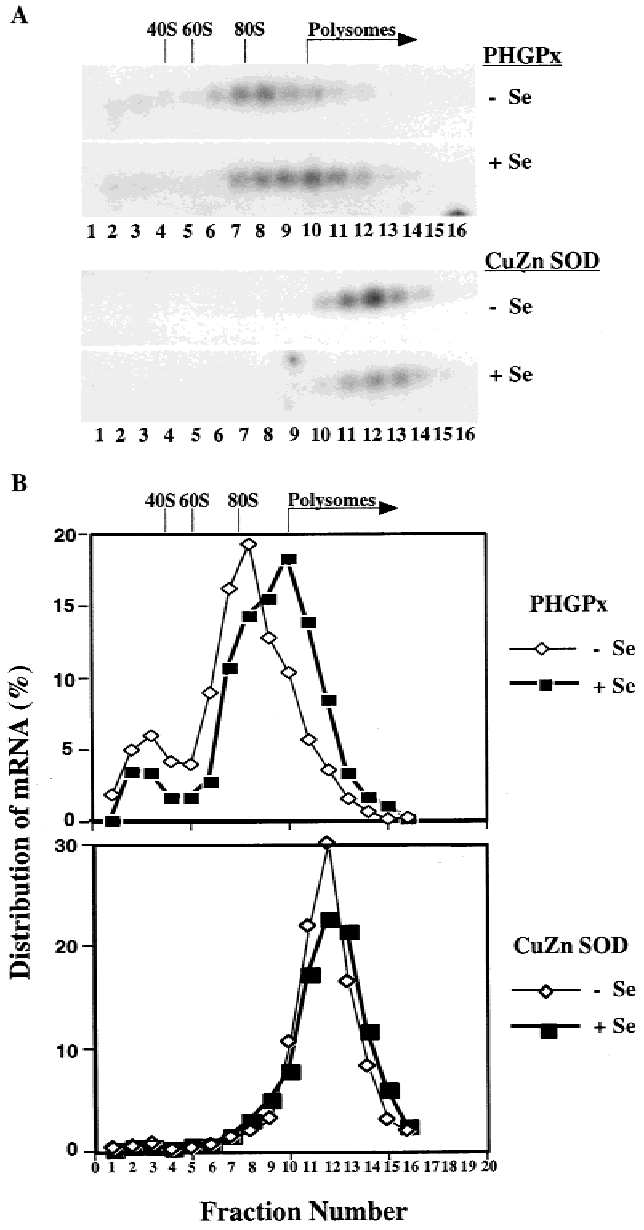


**FIGURE 2.** Effect of selenium supplementation on polysome distribution. Cytoplasmic extracts were made from McArdle 7777 cells supplemented with 5 ng/mL sodium selenite (Se+) or from non-supplemented cells (Se−). **A**: Extracts were centrifuged on two separate linear sucrose gradients run in parallel, and the fractions were analyzed for PHGPx (top) and CuZn SOD (bottom) mRNAs by Northern blotting. **B**: The results are expressed as percent distribution as determined by PhosphorImager analysis. The peaks for the positions of the 40S (fractions 3–4) and 60S (fractions 5–6) ribosomal subunits, 80S monosomes (fractions 7–9), and polysomes (fractions 10–16) are indicated.

## Polysome distribution of PHGPx mRNA in mouse liver extracts

Most studies on Sec insertion have been done with transfected cells where the selenoprotein biosynthetic machinery may be saturated, and there is little information on the efficiency of Sec insertion in vivo. In addition to determining the distribution of endogenous PHGPx mRNA from a cultured cell line, it is important to know if a similar distribution can be observed in tissues. Liver extracts from male mice were layered onto linear sucrose gradients, and the distributions of the endogenous PHGPx and CuZn SOD mRNAs were analyzed. The comparison of the distribution of PHGPx and CuZn SOD mRNAs is shown by the Northern blots in Figure 3A. The Northern results were quantified by PhosphorImager analysis and percent distribution of the mRNAs is plotted in Figure 3B. The peak of PHGPx mRNA abundance was in fractions 10 and 11, whereas the CuZn SOD mRNA sedimented in fractions 11–13 in the polysome region. Thus, in both McArdle 7777 cell and mouse liver extracts, PHGPx mRNA sediments more slowly than expected.

## Effects of mutations at the UGA/Sec codon in PHGPx mRNA on the polysomal distribution in reticulocyte lysates

Low ribosome loading onto an mRNA may be due to inefficient initiation or elongation. To test the hypothesis that there is a defect in elongation at the UGA/Sec codon, we analyzed the polysome distribution of wild-type and mutant PHGPx mRNAs translated in vitro. Figure 4A illustrates the PHGPx constructs used in these experiments. These include a wild-type PHGPx (P/UGA/wt); a cysteine mutant (P/UGU/wt) in which the UGA/Sec codon is replaced with UGU/Cys; a SECIS element deletion mutant (P/UGA/Δmut) in which the AUGA element is deleted from the 3′UTR; and a mutant in which UGA/Sec is replaced with a UAA stop codon (P/UAA/wt). The wild-type and mutant RNAs were translated in a modified rabbit reticulocyte lysate system that we recently developed to analyze the incorporation of Sec into selenoproteins in vitro (Copeland et al., 2000). Translation of PHGPx mRNA in this system is both SBP2 and SECIS element dependent. In the present study, the assay conditions were modified specifically for polysome analysis. $^{32}$P-labeled RNAs were translated for 25 min at 37 °C in the presence of $^{35}$S methionine as described in Materials and Methods. The translation products were analyzed by SDS-PAGE (Fig. 4B), and the polysome distributions of the mRNAs were analyzed by linear sucrose gradients (Fig. 5).

As shown in Figure 4B, the UGU/Cys mutant (lane 5) was translated ~100 times more efficiently than the wild-type PHGPx mRNA (lane 1). No detectable PHGPx was translated from the AUGA deletion mutant (Fig. 4B, lane 3) or the UAA/Stop codon mutant (Fig. 4B, lane 7) mRNAs. Interestingly, we did not detect any truncated translation products for the wild-type PHGPx, AUGA deletion mutant, or the UAA/Stop mutant mRNAs under our experimental conditions. The inability to detect the truncated product may be due to its instability in the

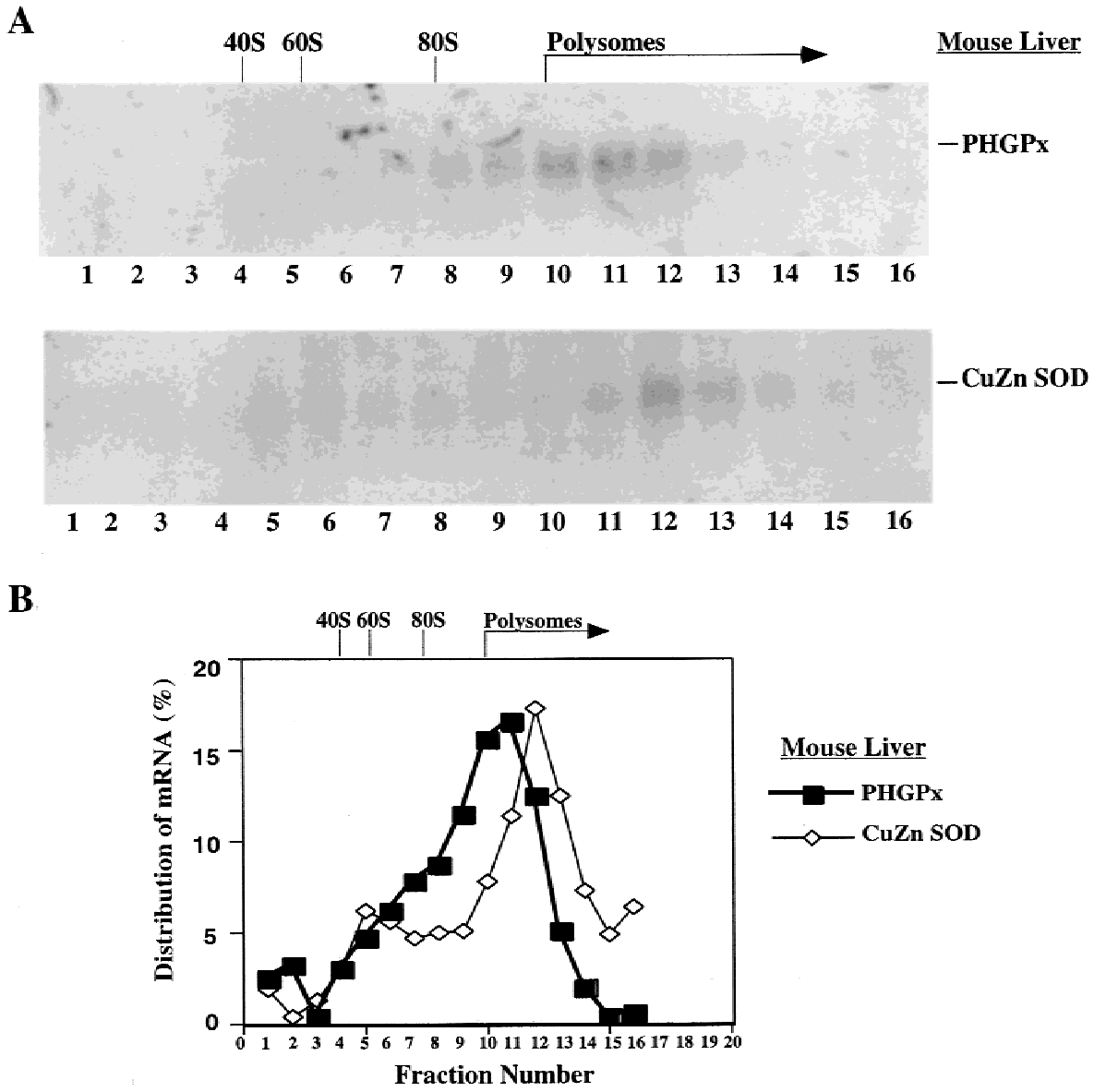


**FIGURE 3.** Polysome distribution of PHGPx and CuZn SOD mRNAs in mouse liver extracts. **A**: Mouse liver extracts were layered onto linear sucrose gradients, and the fractions were analyzed for PHGPx (top) and CuZn SOD (bottom) mRNAs by Northern blotting. **B**: The results are expressed as percent distribution as determined by PhosphorImager analysis. The positions of the ribosomal subunits 40S (fractions 3–4) and 60S (fractions 5–6) ribosomal subunits, monosomes (fractions 7–9), and polysomes (fractions 10–16) are indicated.

reticulocyte lysate, a finding that was reported previously for GPx (Jung et al., 1994).

For polysome analysis, the translation reactions were analyzed on separate linear sucrose gradients that were fractionated in parallel. Because the $A_{254}$ profiles from reticulocyte lysates only exhibit absorbances for the 60S and 80S peaks, McArdle cell cytoplasmic extracts were added to the reticulocyte lysate reactions prior to centrifugation to provide markers for polysome size. A representative profile is shown in Figure 5A in which 60S subunits, monosomes, and polysomes with increasing numbers of ribosomes are resolved. From six separate profiles, we determined the average fraction number for the 60S (4.4 ± 0.11) and 80S (6.99 ± 0.06) peaks, the starting fraction at which polysomes were detected (9.7 ± 0.12), and the peak where disomes sediment (10.51 ± 0.17).

To analyze the distribution of the wild-type and mutant RNAs, the gradient fractions were extracted with Trizol and isolated on a 4% acrylamide gel (Fig. 5B). Each mRNA exhibited a large initial peak in the 40S and 60S regions of the gradient. This was not due to RNA degradation, because the mRNAs maintained their integrity throughout the gradient (Fig. 5B). The large initial peak was seen with all mRNAs that were tested, including nonselenoprotein mRNAs (data not shown),

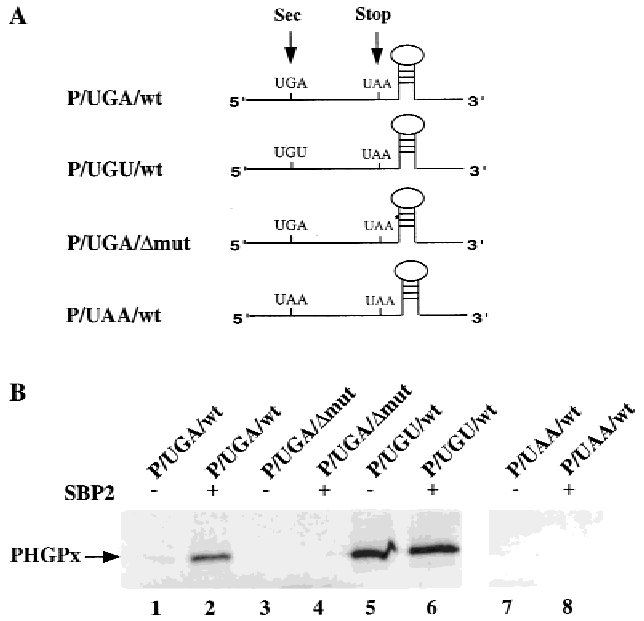


**FIGURE 4.** Analysis of mutant PHGPx mRNAs. **A**: A diagram of the PHGPx constructs used in this study. **B**: PHGPx mRNAs diagramed in **A** were labeled with $^{32}$P-UTP, quantitated, and added to reticulocyte lysates in the presence of $^{35}$S-Met. Recombinant C-terminal SBP2 protein (125 ng) was added to the reactions in lanes 2, 4, 6, and 8. The in vitro translated PHGPx protein was purified by BSP-agarose as described in Materials and Methods, resolved by electrophoresis, and detected by PhosphorImager analysis. The position of the PHGPx protein is indicated on the left.

and it appears to be a characteristic of the reticulocyte lysates when used for polysome analysis (Grafi et al., 1993). In the polysome region of the gradient, the wild-type PHGPx mRNA peaked in fractions 9 and 10 (Fig. 5B), which is similar to the results that were obtained with hepatoma cell and liver extracts. One possible explanation for this low sedimentation velocity of the wild-type PHGPx mRNA is that the mRNA may be associated with large ribonucleoprotein (RNP) particles. To address this possibility, translation reactions were treated prior to centrifugation with 30 mM EDTA, which chelates $Mg^{2+}$ and causes the release of mRNAs from ribosomes due to dissociation of ribosomal subunits. The addition of EDTA shifted all of the wild-type PHGPx mRNA to the large peak near the top of the gradient (data not shown). These results suggest that the PHGPx mRNA in fractions 9 and 10 is associated with ribosomes, rather than with large RNP particles. As shown in Figure 5B, the P/UAA/wt and P/UGA/Δmut mRNAs showed a distribution similar to the wild-type mRNA in the polysome region of the gradient, with peaks in fractions 9 and 10. In contrast, the P/UGU/wt mRNA exhibited a broader distribution, sedimenting in fractions 9–13. The increased loading of ribosomes on the UGU/Cys mutant mRNA is consistent with the increased translation of this mRNA shown in Figure 4B.

## Effect of SBP2 on translation and polysome distribution

We have shown previously that SBP2 is limiting in reticulocyte lysates and that the C-terminal fragment of SBP2 is sufficient to increase translation of PHGPx mRNA in vitro (Copeland et al., 2000). Using the conditions specific for polysome analysis, the wild-type and mutant PHGPx mRNAs were translated in vitro in the presence 125 ng of recombinant C-terminal SBP2 protein. When the C-terminal SBP2 protein was added to the reaction, the translation of the wild-type P/UGA/wt mRNA was stimulated 25-fold (Fig. 4B, lanes 1 and 2). Reticulocyte lysate reactions with or without the addition of SBP2 protein were used to analyze the polysomes translating $^{32}$P-labeled P/UGA/wt, P/UAA/wt, P/UGA/Δmut, and P/UGU/wt RNAs. The reactions were analyzed on separate sucrose gradients that were run in parallel. The distribution of each mRNA was determined by direct Cerenkov counting of the gradient fractions, and a representative set of plots is shown in Figure 6. The experiments were repeated three times to calculate the percentage of each RNA in different regions of the gradient, and the results for the association with moderately heavy polysomes (fractions 12–16) are shown in Figure 7.

The results obtained by direct Cerenkov counting of the gradient fractions (Fig. 6) were consistent with those obtained by PhosphorImager analysis of the RNA gels (data not shown). Although there was some variability between experiments in the amplitudes of the large initial peak, there was not a statistically significant difference between the wild-type and mutant RNAs in their association with the 40S and 60S peaks ($n = 3$). The P/UGU/wt (Fig. 6A), P/UGA/Δmut (Fig. 6C), and P/UAA/wt RNAs (Fig. 6D) had similar polysome profiles, peaking in fraction 9 with very little RNA in the later fractions of the gradient. In contrast, the P/UGU/wt RNA showed a second polysomal peak in fraction 12, in addition to a peak at fraction 9 (Fig. 6B). As shown in Figure 7, there was a significant increase ($p < 0.004$) in the percentage of P/UGU/wt RNA associated with heavier polysomes compared to P/UGA/wt, P/UAA/wt, and P/UGA/Δmut RNAs.

In the presence of SBP2, wild-type P/UGA/wt mRNA sediments to a heavier region of the sucrose gradient, consistent with an increase in ribosome loading (Fig. 6A). As shown in Figure 4B, SBP2 had no effect on the translation of the mutant PHGPx mRNAs, P/UGU/wt (lanes 3 and 4), P/UGA/Δmut (lanes 5 and 6), and P/UAA/wt (lanes 7 and 8). SBP2 also did not increase ribosome loading on the mutant mRNAs (Figs. 6B,C,D and 7). The percentage of P/UGA/wt RNA associated with moderately heavy polysomes in the presence of SBP2 was not significantly different than the percentage of P/UGU/wt RNA (Fig. 7). These results suggest that SBP2 may increase the effi-

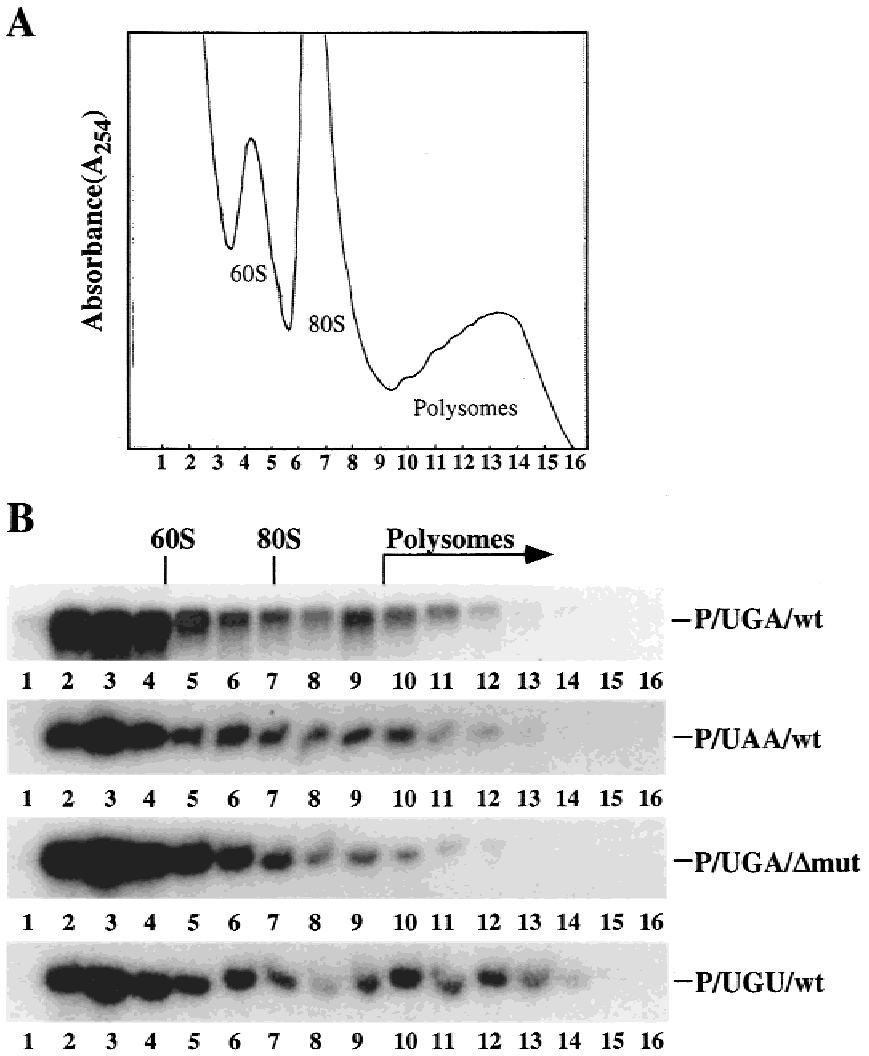


**FIGURE 5.** Polysome analysis of PHGPx mutants. **A**: A typical absorbance profile of reticulocyte lysate with McArdle extract added to provide markers for polysome size. Fraction numbers were assigned for the 60S (4.4 ± 0.11) and 80S (6.99 ± 0.06) ribosomal subunits, the start of the polysomes (9.7 ± 0.12), and the disome peak (10.51 ± 0.17) by averaging the peaks from six reticulocyte/McArdle extract absorbance profiles. **B**: $^{32}$P-labeled P/UGA/wt, P/UAA/wt, P/UGA/Δmut, and P/UGU/wt RNAs were translated in vitro in reticulocyte lysate and the reactions were run on separate linear sucrose gradients that were fractionated in parallel. The RNAs were isolated from each fraction, resolved on 4% polyacrylamide gels, and analyzed by autoradiography. The positions of the average peaks for the 60S (fraction 4.4) and 80S (fraction 6.99) ribosomal subunits and the start of the polysomes (fraction 9.7) are indicated, as described in **A**.

ciency of PHGPx translation by enhancing readthrough of the UGA/Sec codon.

## DISCUSSION

Although we are beginning to have a better understanding of the *trans*-acting factors involved in eukaryotic Sec insertion, little information has been presented about the polysomes that translate mammalian selenoprotein mRNAs. In this study, we show that PHGPx mRNA is partially loaded with ribosomes for the length of its coding region. The association of PHGPx mRNA with a small complex of 1–2 ribosomes was observed in McArdle 7777 cells, in mouse liver, and in in vitro translation reactions. The frequency of initiation is often the rate-limiting step in translation. However, our results support the hypothesis that elongation is impeded at the UGA/Sec codon, leading to the inefficient translation of selenoprotein mRNAs. Although the translation start site of PHGPx mRNA is less than favorable with a T at +4, it does have an A at position −3 as well as a 7/10 match with the Kozak consensus sequence. In addition, the P/UGU/Cys RNA does not appear to be inefficiently translated in reticulocyte lysate or transfected cells compared to other mRNAs (data not shown). It is important to note that although the sequence contexts for the translation start sites of the wild-type and UGU/Cys mRNAs are identical, we cannot formally ex-

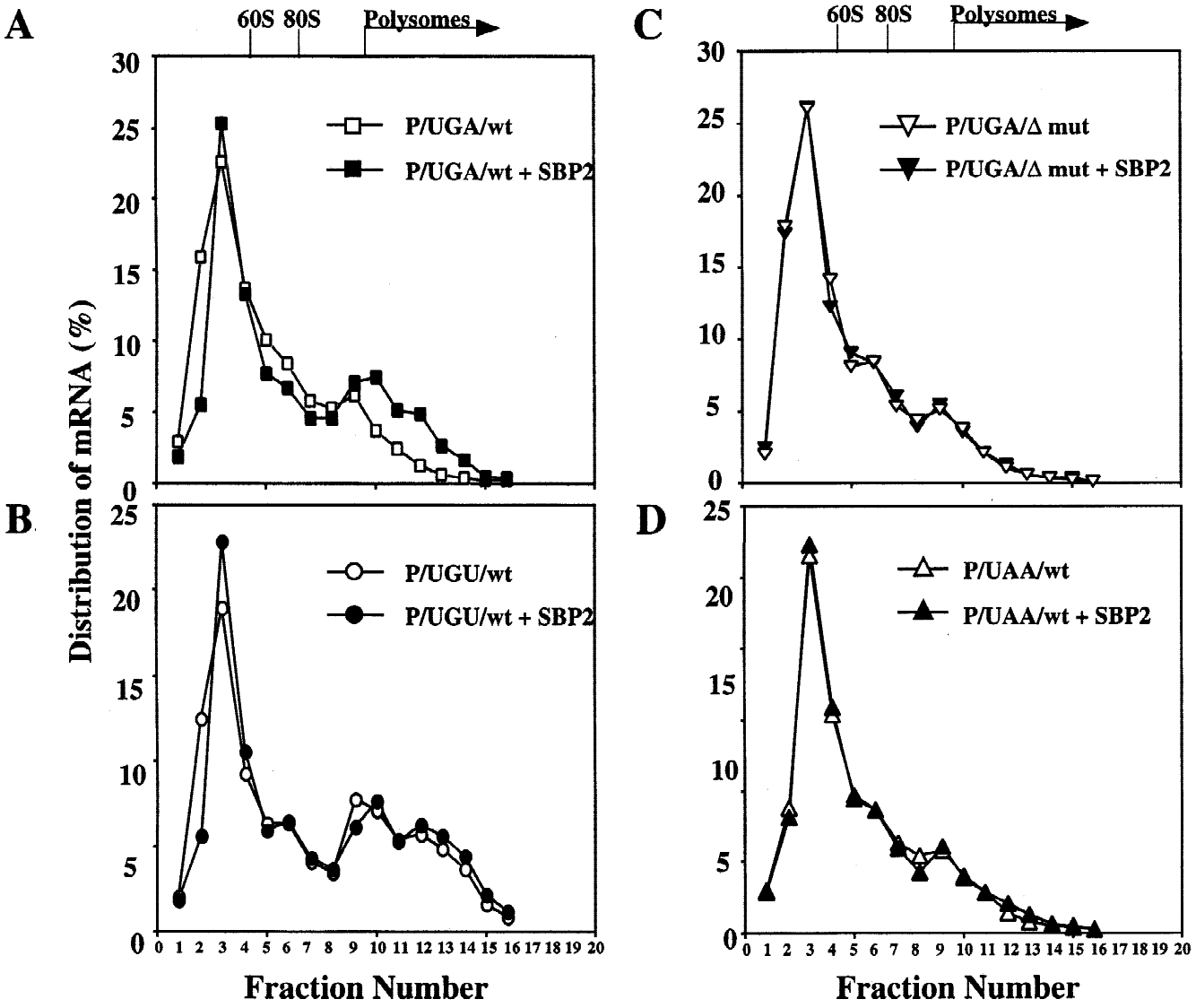


**FIGURE 6.** Effect of SBP2 on the polysome distribution of wild-type and mutant PHGPx mRNAs. $^{32}$P-labeled wild-type and mutant PHGPx mRNAs were translated in the presence or absence of 125 ng of C-terminal SBP2 protein. The translation reactions were analyzed in 15–50% sucrose gradients, and the distribution of $^{32}$P-labeled mRNAs was determined. The figure shows a representative set of plots for the polysome distribution of P/UGA/wt (**A**), P/UGU/wt (**B**), P/UGA/Δmut (**C**), and P/UAA/wt (**D**) mRNAs. The positions of the 60S (4.4 ± 0.11) and 80S (6.99 ± 0.06) peaks and the start of the polysomes (9.7 ± 0.12) are indicated, as described in the legend to Figure 5.

clude some contribution of initiation to the slow sedimentation velocity of wild-type PHGPx mRNA.

Mammalian selenoprotein biosynthesis is regulated by the availability of several factors, including selenium, Sec-tRNA$^{Sec}$, and SBP2. We found that selenium supplementation of McArdle 7777 cells increased the loading of ribosomes onto PHGPx mRNA, but not CuZn SOD mRNA. This result is in agreement with a previous study that showed that GPx mRNA is associated with a larger polyribosomal complex in cells supplemented with selenomethionine, compared to untreated cells (Jornot & Junod, 1995). Even in selenium supplemented McArdle 7777 cells, PHGPx mRNA still sediments to a lighter portion of the gradient compared to CuZn SOD mRNA, which has a coding region of similar size. We speculate that the availability of selenium may increase the production of the Sec-tRNA$^{Sec}$, promoting Sec insertion, but that other components in this pathway may still be limiting.

It is well documented that changing the UGA/Sec codon to UGU/Cys results in a dramatic increase in selenoprotein production. However, there was no direct evidence until now that this increase occurred at the translational level. For example, the wild-type protein may be less stable than the Cys-containing mutant protein. Because selenoprotein synthesis is inefficient in transfected cells, we took advantage of the recently developed in vitro system for translating selenoprotein

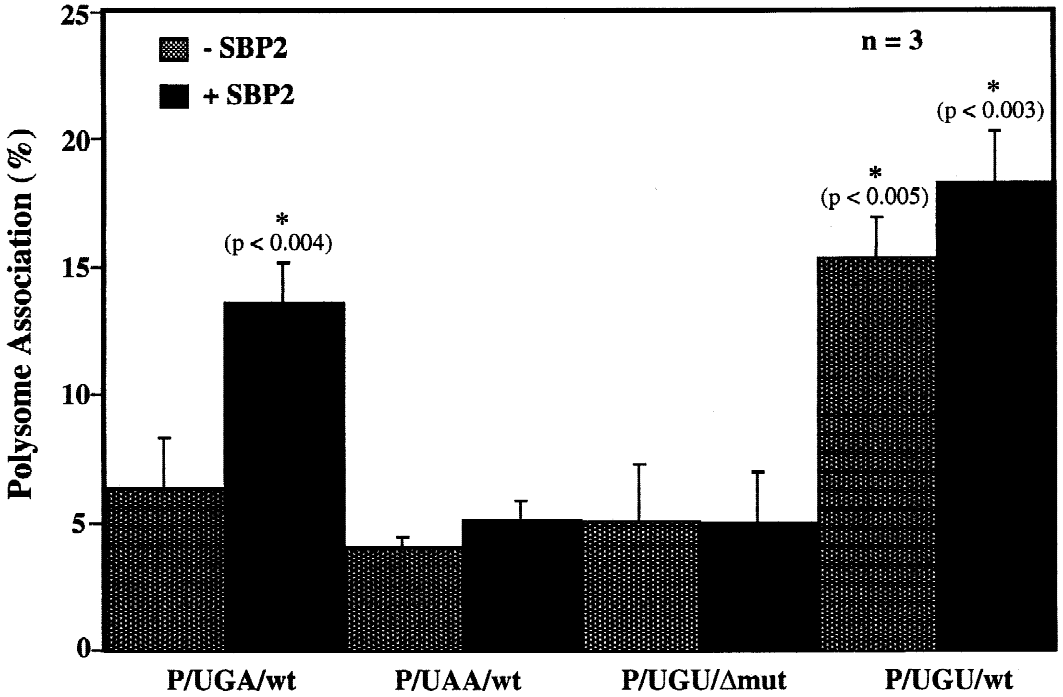


**FIGURE 7.** Polysome association of wild-type and mutant PHGPx mRNAs. The graph shows the average percent polysome association in the moderate to heavily loaded portion of the gradient (fractions 12–16) for the wild-type and mutant PHGPx mRNAs in the presence or absence of 125 ng of C-terminal SBP2 protein ($n = 3$). The results were analyzed using a two sample *t*-test and statistically significant differences compared to the P/UGA/wt RNA are indicated by the asterisks.

mRNAs (Copeland et al., 2000), which allowed us to analyze the polysome distribution of wild-type and mutant PHGPx mRNAs. Mutation of UGA/Sec to UGU/Cys resulted in a shift of the mRNA to the polysome-rich region of the gradient, which correlated with an increase in translational efficiency. Thus, there is a defect in elongation at the UGA/Sec codon, which may explain why Sec insertion is less efficient than the incorporation of standard amino acids. Mutant mRNAs in which UGA/Sec was replaced with a UAA stop codon or in which the SECIS element core was deleted were translated more poorly than the wild-type PHGPx mRNA. However, there were no statistically significant differences between the polysome profiles of the wild-type RNA and the UAA/Stop and SECIS mutant RNAs. We were also unable to detect a truncated product translated from the wild-type and UAA/Stop RNAs. Thus, our results do not allow us to distinguish whether termination is more efficient at a UAA stop codon than at the UGA/Sec codon, or whether the ribosome pauses or terminates at UGA/Sec. If termination at UGA/Sec was less efficient than initiation, one might expect to see stacking of ribosomes on the wild-type PHGPx RNA. However, ribosomal stacking has only been studied in a few cases. Wolin and Walter (1988) provided evidence for pausing of the 80S monosome after assembly as the rate-limiting step in the elongation reaction. Depending on the rate of elongation, the distance between the AUG and the UGA/Sec codon in PHGPx mRNA (135 nt) may not be sufficiently long to allow ribosomes to stack. Alternatively, if the ribosome terminates efficiently at the UGA/Sec codon, there would be less opportunity for ribosomal stacking.

Another factor that we tested was SBP2, which is required for Sec incorporation and is limiting in reticulocyte lysates (Copeland et al., 2000). If the machinery for Sec insertion signals the ribosome to pause at the UGA/Sec codon, the availability of SBP2 protein may relieve this pause and enhance elongation. We found that the addition of SBP2 to in vitro translation assays resulted in the association of the wild-type PHGPx mRNA with a larger polyribosomal complex. This effect of SBP2 was UGA/Sec codon and SECIS element dependent. SBP2 did not increase the translation or ribosome loading of mutant RNAs that contained UGU/Cys or UAA/Stop in place of the UGA/Sec codon, or that had a deletion in the SECIS element core. We propose a model in which SBP2 facilitates elongation at the UGA/Sec codon by blocking termination and allowing for the delivery of the Sec-tRNA$^{Sec}$ to the A site of the ribosome. Interestingly, even in the presence of SBP2, the wild-type PHGPx mRNA is consistently translated approximately four- to fivefold less efficiently than the UGU/Cys mutant. Preliminary results indicate that the Sec-tRNA$^{Sec}$ is not limiting in reticulocyte lysates (P.R. Copeland and D.M. Driscoll, unpubl. observations). However, the rate at which Sec-tRNA$^{Sec}$ is delivered to the ribosome may rely on other, as yet

unidentified factors. One of these factors may be the mammalian homolog of SELB, the prokaryotic Sec-specific elongation factor. SELB is a multifunctional protein, which binds to both the Sec-tRNA$^{Sec}$ and to the b-SECIS element in the selenoprotein mRNA. Because SBP2 is a SECIS-binding protein but not an elongation factor, the functional activity of SELB may be encoded by two distinct polypeptides in mammals. As new components involved in the Sec machinery are identified, the ability to test these new and existing factors using reticulocyte lysates in conjunction with polysome analysis will greatly enhance our understanding of the mechanism of Sec insertion.

## MATERIALS AND METHODS

### Preparation of cytoplasmic extracts from cultured cells

Flasks of McArdle 7777 cells were grown in media containing 10% fetal bovine calf serum (FBS) or 10% FBS with 5 ng/mL sodium selenite. Cells were harvested by trypsinization followed by centrifugation, and washed with 10 mL ice-cold phosphate-buffered saline (PBS) containing 50 $\mu$g/mL cycloheximide. After the addition of cycloheximide, experimental conditions were maintained at 4 °C. Cell lysates were made according to the method of Chen et al. (1993b). Aliquots (0.5 mL) of the lysates, equivalent to material from $4 \times 10^7$ cells, were layered onto 15–50% (w/v) linear sucrose gradients as described below.

### Preparation of cytoplasmic extracts from mouse liver

Male mice were sacrificed, and the livers were removed and placed in 4 vol of homogenizing buffer (0.25 M sucrose, 20 mM HEPES, pH 7.5, 250 mM KCL, 5 mM $MgCl_2$, 2 mM dithiothreitol, 150 $\mu$g/mL cycloheximide, and 1 mg/mL sodium heparin) at 4 °C. After the addition of cycloheximide, the experimental conditions were maintained at 4 °C. The tissue was homogenized with five stokes using a high-clearance Dounce homogenizer. After mixing with a 10% (v/v) solution of the detergent Triton X-100 to a final concentration of 1% (v/v), the homogenate was centrifuged at 14,000 $\times$ *g* at 4 °C for 10 min. Aliquots of the supernatant (0.5 mL) were layered onto linear 15–50% (w/v) sucrose gradients.

### Sucrose gradient preparation and analysis

Linear 15–50% (w/v) sucrose gradients (11 mL) were prepared by two methods as described by Abe & Davies (1986) or Chen et al. (1993b). Extracts or in vitro translation reactions (0.5 mL) were layered on top of the gradients, and the gradients were centrifuged at 40,000 rpm for 120 min at 4 °C in a Beckman SW 41 rotor. To provide markers for polysome size, 250 $\mu$L aliquots of McArdle cell extract were added to some reticulocyte lysate reactions before layering onto the gradients. Using a BioCad Sprint (PE Biosystems) perfusion chromatography system, gradient fractions (0.6 mL) were collected by upward displacement with 60% sucrose solution into Eppendorf tubes. The absorbance profile (254 nm) of the gradients was recorded during the collection of fractions. Assignments of the 40S, 60S, and 80S peaks and polysomes were based on the absorbance profile and the distribution of the 18S and 28S ribosomal rRNAs in the gradient fractions. For cell extracts and liver extracts, collection tubes contained 6 $\mu$L 10% SDS and 3 $\mu$L 10 mg/mL Proteinase K, and the fractions were heated at 55 °C for 30 min. After heating, each fraction was extracted with phenol/chloroform/isoamyl alcohol (25:24:1), and the RNA in each fraction was precipitated with absolute ethanol and 3 M sodium acetate (pH 5.2) overnight at −20 °C. The precipitated RNA was collected by centrifugation (12,000 rpm, 10 min, 4 °C), washed with 70% ethanol, and dried at room temperature. Pellets were dissolved in sterile water and analyzed as described below. For in vitro translation reactions, the gradient fractions were collected and the tubes were counted directly by the Cerenkov counting method.

### RNA analysis

RNAs from the gradient fractions were denatured with formaldehyde and formamide, and separated by electrophoresis in 1.2% agarose, 2 M formaldehyde gels. The 18S and 28S ribosomal RNAs were detected by ethidium bromide staining. Gels were transferred to nylon membranes. Blots were probed with a $^{32}$P-$\gamma$-dCTP random primed PHGPx, GPx, CuZn SOD, and GAPDH probes (RadPrime, Life Technologies) corresponding to the coding region for each using Expresshyb (Clontech) hybridization solution and conditions as described by manufacturer. $^{32}$P-labeled RNA from the reticulocyte lysate gradient fractions was extracted with Trizol (Gibco/BRL), precipitated, and run on 4% polyacrylamide gels. Both the blots and gels were quantified by PhosphorImager (Molecular Dynamics) analysis.

### Constructs and in vitro transcription

Constructs for the PHGPx wild-type RNA and mutants were made as described (Copeland et al., 2000). For replacing the UGA/Sec codon with a UAA/Stop codon, an Altered Sites Mutagenesis kit (Promega) was used to perform site-directed mutagenesis using the mutagenic oligonucleotide GGCCTCG CAA**TA**AGGCAAAACCG (altered nucleotides in boldface). Verification of all constructs was performed by DNA sequencing. Prior to transcription, plasmid DNAs were linearized with *Xba*I. Transcripts were made in the presence of 5 $\mu$Ci $^{32}$P-UTP by in vitro transcription (Ribomax T7, Promega). Also included in the reactions was $^{m}$7GpppG (Roche) for the synthesis of capped mRNA.

### In vitro translation

$^{32}$P-UTP-labeled, capped, polyadenylated PHGPx mRNAs were generated by Ribomax T7 (Promega) in vitro transcription from *Xba*I-linearized plasmid DNAs. In vitro translation reactions were the same as described (Copeland et al., 2000) except for the following changes. Reactions included $^{35}$S methionine instead of $^{75}$Se-labeled Sec-tRNA$^{Sec}$ and incubation time was shortened from 45 min to 25 min at 37 °C. For

analysis of $^{35}$S labeled proteins, 25 $\mu$L reactions were terminated by the addition of 250 $\mu$L PBS containing 2.5 mM DTT and 25 $\mu$L of BSP-agarose (Sigma). This mixture was incubated for 1 h at 4 °C, beads were washed with PBS/DTT and protein eluted in SDS sample buffer followed by separation by 15% SDS-PAGE. Radiolabeled PHGPx was detected by PhosphorImager analysis. For polysome analysis, the volume of the translation reactions was increased to 100 $\mu$L. Incubation temperature and time remained the same as stated above. After incubation, 400 $\mu$L ice-cold gradient buffer containing 0.1 mg/mL cycloheximide was added, and the total volume of 0.5 mL was layered onto 15–50% linear sucrose gradients. After the addition of cycloheximide, experimental conditions were maintained at 4 °C.

### SBP2 purification

Recombinant C-terminal SBP2 protein purification was performed as described by Copeland et al. (2000), except that the elution buffer was exchanged to 20 mM Tris-Acetate, pH 7.5, 50 mM KoAc using a 10 × 100 mm Fast Desalting column (Pharmacia).

## ACKNOWLEDGMENTS

We thank Jeff Kniele for technical assistance in the early phases of this work. This research was supported by Public Health Service Grants HL29582 (D.M.D.) and F32 DK09878 (P.R.C.) from the National Institutes of Health.

*Received March 9, 2000; returned for revision*
*April 5, 2000; revised manuscript received July 28, 2000*

## REFERENCES

Abe S, Davies E. 1986. Quantitative analysis of polysomes using a baseline from uncentrifuged blank gradients. *Memoirs of the College of Agriculture, Ehime University 31*:187–199.

Baron C, Heider J, Bock A. 1993. Interaction of translation factor SELB with the formate dehydrogenase H selenopolypeptide mRNA. *Proc Natl Acad Sci USA 90*:4181–4185.

Bermano G, Nicol F, Dyer JA, Sunde RA, Beckett GJ, Arthur JR, Hesketh JE. 1996. Selenoprotein gene expression during selenium-repletion of selenium-deficient rats. *Biol Trace Elem Res 51*:211–223.

Berry MJ, Banu L, Chen YY, Mandel SJ, Kieffer JD, Harney JW, Larsen PR. 1991. Recognition of UGA as a selenocysteine codon in type I deiodinase requires sequences in the 3′ untranslated region. *Nature 353*:273–276.

Berry MJ, Harney JW, Ohama T, Hatfield DL. 1994. Selenocysteine insertion or termination: Factors affecting UGA codon fate and complementary anticodon:codon mutations. *Nucleic Acids Res 22*:3753–3759.

Berry MJ, Maia AL, Kieffer JD, Harney JW, Larsen PR. 1992. Substitution of cysteine for selenocysteine in type I iodothyronine deiodinase reduces the catalytic efficiency of the protein but enhances its translation. *Endocrinology 131*:1848–1852.

Chen GF, Fang L, Inouye M. 1993a. Effect of the relative position of the UGA codon to the unique secondary structure in the fdhF mRNA on its decoding by selenocysteinyl tRNA in *Escherichia coli. J Biol Chem 268*:23128–23131.

Chen X, Sparks JD, Yao Z, Fisher EA. 1993b. Hepatic polysomes that contain apoprotein B mRNA have unusual physical properties. *J Biol Chem 268*:21007–21013.

Copeland PR, Driscoll DM. 1999. Purification, redox sensitivity, and RNA binding properties of SECIS-binding protein 2, a protein involved in selenoprotein biosynthesis. *J Biol Chem 274*:25447–25454.

Copeland PR, Fletcher JE, Carlson BA, Hatfield DL, Driscoll DM. 2000. A novel RNA binding protein, SBP2, is required for the translation of mammalian selenoprotein mRNAs. *EMBO J 19*: 306–314.

Ehrenreich A, Forchhammer K, Tormay P, Veprek B, Bock A. 1992. Selenoprotein synthesis in *E. coli.* Purification and characterisation of the enzyme catalysing selenium activation. *Eur J Biochem 206*:767–773.

Forchhammer K, Bock A. 1991. Selenocysteine synthase from *Escherichia coli*. Analysis of the reaction sequence. *J Biol Chem 266*:6324–6328.

Gladyshev VN, Hatfield DL. 1999. Selenocysteine-containing proteins in mammals. *J Biomed Sci 6*:151–160.

Grafi G, Sela I, Galili G. 1993. Translational regulation of human interferon mRNA: Association of the 3′ AU-rich sequence with the poly(A) tail reduces translation efficiency in vitro. *Mol Cell Biol 13*:3487–3493.

Heider J, Baron C, Bock A. 1992. Coding from a distance: Dissection of the mRNA determinants required for the incorporation of selenocysteine into protein. *EMBO J 11*:3759–3766.

Huttenhofer A, Heider J, Bock A. 1996. Interaction of the *Escherichia coli* fdhF mRNA hairpin promoting selenocysteine incorporation with the ribosome. *Nucleic Acids Res 24*:3903–3910.

Jornot L, Junod AF. 1995. Differential regulation of glutathione peroxidase by selenomethionine and hyperoxia in endothelial cells. *Biochem J 306*:581–587.

Jung J, Karoor V, Sandbaken MG, Lee BJ, Ohama T, Gesteland RF, Atkins JF, Mullenbach GT, Hill KE, Wahba AJ, Hatfield DL. 1994. Utilization of Selenocysteyl-tRNA$^{[Ser]Sec}$ and seryl-tRNA$^{[Ser]Sec}$ in protein synthesis. *J Biol Chem 269*:29739–29745.

Kim IY, Stadtman TC. 1995. Selenophosphate synthetase: Detection in extracts of rat tissues by immunoblot assay and partial purification of the enzyme from the archaean *Methanococcus vannielii. Proc Natl Acad Sci USA 92*:7710–7713.

Kleene KC. 1993. Multiple controls over the efficiency of translation of the mRNAs encoding transition proteins, protamines, and the mitochondrial capsule selenoprotein in late spermatids in mice. *Dev Biol 159*:720–731.

Lee BJ, Kang SG, Hatfield D. 1989. Transcription of *Xenopus* selenocysteine tRNA Ser (formerly designated opal suppressor phosphoserine tRNA) gene is directed by multiple 5′-extragenic regulatory elements. *J Biol Chem 264*:9696–9702.

Lei XG, Evenson JK, Thompson KM, Sunde RA. 1995. Glutathione peroxidase and phospholipid hydroperoxide glutathione peroxidase are differentially regulated in rats by dietary selenium. *J Nutr 125*:1438–1446.

Leinfelder W, Zehelein E, Mandrand-Berthelot MA, Bock A. 1988. Gene for a novel tRNA species that accepts L-serine and cotranslationally inserts selenocysteine. *Nature 331*:723–725.

Lodish HF, Jacobson M. 1972. Regulation of hemoglobin synthesis: Equal rates of translation and termination of alpha and beta globin chains. *J Biol Chem 247*:3622–3629.

Lodish HF, Porter M. 1980. Translational control of protein synthesis after infection by vesicular stomatitis virus. *J Virol 36*:719–733.

Low SC, Berry MJ. 1996. Knowing when not to stop: Selenocysteine incorporation in eukaryotes. *Trends Biochem Sci 21*:203–208.

Low SC, Harney JW, Berry MJ. 1995. Cloning and functional characterization of human selenophosphate synthetase, an essential component of selenoprotein synthesis. *J Biol Chem 270*:21659–21664.

Martin GW, Harney JW, Berry MJ. 1998. Functionality of mutations at conserved nucleotides in eukaryotic SECIS elements is determined by the identity of a single nonconserved nucleotide. *RNA 4*:65–73.

Meyuhas O, Thompson EA, Jr, Perry RP. 1987. Glucocorticoids selectively inhibit translation of ribosomal protein mRNAs in P1789 lymphosarcoma cells. *Mol Cell Biol 7*:2691–2699.

Palmiter RD. 1972. Regulation of protein synthesis in chick oviduct. II. Modulation of polypeptide elongation and initiation rates by estrogen and progesterone. *J Biol Chem 247*:6770–6780.

Rocher C, Faucheu C, Herve F, Benicourt C, Lalanne JL. 1991. Cloning of murine SeGpx cDNA and synthesis of mutated GPx proteins in *Escherichia coli. Gene 98*:193–200.

Roveri A, Casasco A, Maiorino M, Dalan P, Calligaro A, Ursini F. 1992. Phospholipid hydroperoxide glutathione peroxidase of rat testis. Gonadotropin dependence and immunocytochemical identification. *J Biol Chem 267*:6142–6146.

Roveri A, Maiorino M, Ursini F. 1994. Enzymatic and immunological measurements of soluble and membrane-bound phospholipid-hydroperoxide glutathione peroxidase. *Methods Enzymol 233*: 202–212.

Shen Q, Chu FF, Newburger PE. 1993. Sequences in the 3′-untranslated region of the human cellular glutathione peroxidase gene are necessary and sufficient for selenocysteine incorporation at the UGA codon. *J Biol Chem 268*:11463–11469.

Stadtman TC. 1996. Selenocysteine. *Annu Rev Biochem 65*:83–100.

Thomas JP, Geiger PG, Maiorino M, Ursini F, Girotti AW. 1990. Enzymatic reduction of phospholipid and cholesterol hydroperoxides in artificial bilayers and lipoproteins. *Biochim Biophys Acta 1045*:252–260.

Ursini F, Heim S, Kiess M, Maiorino M, Roveri A, Wissing J, Flohe L. 1999. Dual function of the selenoprotein PHGPx during sperm maturation. *Science 285*:1393–1396.

Walczak R, Carbon P, Krol A. 1998. An essential non-Watson–Crick base pair motif in 3′ UTR to mediate selenoprotein translation. *RNA 4*:74–84.

Walczak R, Westhof E, Carbon P, Krol A. 1996. A novel RNA structural motif in the selenocysteine insertion element of eukaryotic selenoprotein mRNAs. *RNA 2*:367–379.

Wolin SL, Walter P. 1988. Ribosome pausing and stacking during translation of a eukaryotic mRNA. *EMBO J 7*:3559–3569.

Zinoni F, Heider J, Bock A. 1990. Features of the formate dehydrogenase mRNA necessary for decoding of the UGA codon as selenocysteine. *Proc Natl Acad Sci USA 87*:4660–4664.